Zurich, June 15-17 2016
Sustainable Built Environment (SBE) Regional Conference

Expanding Boundaries:
Systems Thinking for the Built Environment

# ECO-MECHANICAL PERFORMANCES OF UHP-FRCC: MATERIAL VS. STRUCTURAL SCALE ANALYSIS

A.P. Fantilli[1]*, S. Kwon[2], H. Mihashi[2], T. Nishiwaki[2]

[1] Politecnico di Torino, Corso Duca degli Abruzzi 24, Torino 10129, Italy
[2] Tohoku University, 6-6, Aoba, Aramaki, Aoba-ku, Sendai, Miyagi 980-8579, Japan
*Corresponding author; e-mail: alessandro.fantilli@polito.it

**Abstract**

One of the big challenges of the construction industry is to reduce the use of cement in new concrete structures for environmental purposes. Ultra-High Performance Fiber-Reinforced Cementitious Composites (UHP-FRCC) can reduce such impact, although the cement content per unit volume is higher than conventional concrete. Due to the high strength and high energy absorption capacity of UHP-FRCC, a reduction of the total amount of structural concrete, and consequently a reduction of cement, can be achieved. However, the results of the sustainability analysis depend on the scale of observation. For this reason, a more effective procedure to evaluate the eco-mechanical performance is herein introduced with the aim of tailoring eco-friendly cement-based composites. The proposed approach has been applied to some UHP-FRCCs containing wollastonite microfibers, which remarkably improve the mechanical performances at structural scale level, without increasing the environmental impact of the materials.

**Keywords:**

Ultra High-Performance Fibre-Reinforced Cementitious Composites (UHP-FRCC); Wollastonite microfibers; Eco-Mechanical Performances; Material scale analysis; Structural scale analysis.

## 1 INTRODUCTION

According to Fantilli and Chiaia [1], the best concrete mixture must show the highest Eco-Mechanical Index (*EMI*), in which both the ecological and mechanical aspects are included:

$$EMI = {}^{MI}\!/_{EI} \qquad (1)$$

where *MI* = mechanical index, and *EI* = ecological Index.

To rate these performances in a more comprehensive way, also the non-dimensional diagram illustrated in Fig.1 can be used [2]. In this diagram, $MI_{inf}$ is the lower bound value of the mechanical performances, whereas the upper bound value of the ecological impact is represented by $EI_{sup}$. Both these bounds can be prescribed by code rules, or imposed by tender requirements. Accordingly, four different zones can be detected within the non-dimensional diagram (see Fig.1):

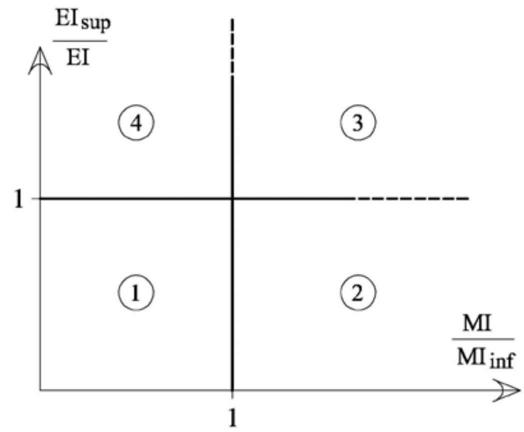


*Fig. 1: The non-dimensional diagram to rate the eco-mechanical performances of cement-based composites.*

- Zone 1: Low mechanical performances– Low ecological performances;

G. Habert, A. Schlueter (eds.): Expanding Boundaries © 2016 vdf Hochschulverlag AG an der ETH Zürich
DOI 10.3218/3774-6_67, ISBN 978-3-7281-3774-6, http://vdf.ch/expanding-boundaries.html

- Zone 2: High mechanical performances–Low ecological performances;
- Zone 3: High mechanical performances–High ecological performances;
- Zone 4: Low mechanical performances–High ecological performances.

The application of the Eco-mechanical analyses to Ultra-High Performance Fiber-Reinforced Cementitious Composites (UHP-FRCC), whose strength and ductility is higher than those of the conventional Fiber-Reinforced Cementitious Composites (FRCC) [3], can appear a pointless academic exercise. As is well known, the content of cement, and of the fibers as well, is remarkably higher, and therefore the environmental impact increases with respect to that of FRCC. Even with the partial substitution of the sand with wollastonite, a natural material capable of increasing the mechanical performances [4], UHP-FRCC cannot be considered as an environmental friendly concrete. This is particularly true when the performances are measured at the material scale [5]. Conversely, the following sections show the better ecological and mechanical performances of a full-scale structural member (i.e., the beam of a frame) made with UHP-FRCC containing wollastonite.

## 2 ANALYSIS AT MATERIAL SCALE

Four UHP-FRCCs are herein investigated. The mix proportions of these composites are shown in Table 1 (where, W = water, B = binder, SP = superplasticizer, D = anti-foaming agent, S = sand, and Wo = wollastonite microfibers). In all the series, 1.5 % of macrofiber (steel-B in Table 2) and 1.0 % of steel mesofibers (steel-A in Table 2) have been added. With respect to the reference composite named U_0, in all the other UHP-FRCC the sand was partially replaced by wollastonite microfibers ($CaSiO_3$) at volume content of 27%. The aspect ratios of the three wollastonite microfibers Wo-1, Wo-2, and Wo-3, added respectively to U_1, U_2 and U_3, were almost the same (see Table 2). The Wo-1 fibers varied in length from 50 and 2,000 μm.

| Series | W/B wt % | SP/B wt % | D/B wt % | S/B wt % | Wo/B wt % |
|---|---|---|---|---|---|
| U_0 | 15 | 1.3 | 0.02 | 48 | - |
| U_1 | | 1.8 | | 35 | 13 |
| U_2 | | | | | |
| U_3 | | 2.1 | | | |

*Table 1: The UHC-FRCC investigated in the present project.*

In addition, Wo-1 varied more in length and diameter with respect to Wo-2 fibers and Wo-3 fibers (Table 2). The densities of the silica sand and of the wollastonite microfibers were 2.6 g/cm$^3$ and 2.9 g/cm$^3$, respectively.

| fiber | Length mm | Φ μm | $f_y$ MPa | $E_s$ GPa |
|---|---|---|---|---|
| Wo-1 | 0.05-2 | - | 2700-4100 | 303-530 |
| Wo-2 | 0.6 | 40 | | |
| Wo-3 | 0.16 | 15 | | |
| steel-A | 6 | 160 | 2000 | 205 |
| steel-B | 30 | 380 | 3003 | |

*Table 2: Properties of the fibres.*

### 2.1 Evaluation of EI

As the definition of *EI* is related to what is generally considered as pollution end/or environmental impact, the following formula is assumed herein:

$$EI = (\alpha \cdot wc_\alpha) \cdot (\beta \cdot wc_\beta) \cdot (\gamma \cdot wc_\gamma) \quad (2)$$

where α = quantity of carbon dioxide ($CO_2$); β = quantity of embodied energy; and γ = volume of water. As the ecological performances are related to the local condition in the place of use [6], three weighting coefficients ($wc_\alpha$, $wc_\beta$, $wc_\gamma$), which can be properly adjusted depending on water shortage, transportation, grabbing of raw materials, etc., are also introduced within Eq.(2). For instance, the longer the distance between concrete plant and building site, the higher the value of $wc_\alpha$ due to the impact of transportation.

The impact of each component, in terms of α, β, and γ, is reported in Table 3. Such values are in accordance with those used by Chiaia et al. [7].

| Components | α kg$CO_2$/kg | β MJ/kg | γ m$^3$ $H_2O$/kg |
|---|---|---|---|
| Cement type | 0.832 | 4.73 | 1.64 |
| Ground limestone | 0.0191 | 0.755 | 1 |
| Fly ash | - | - | - |
| Silica fume | - | - | - |
| Aggregates | 0.00246 | 0.0546 | 0.027 |
| Steel | 1.50 | 20.6 | 2.79 |
| Water | 0.000318 | 0.0057 | 0.01 |
| Wollastonite | 0.0567 | - | - |
| SP | 0.72 | 18.3 | - |
| Air entraining | 0.086 | 2.1 | - |

*Table 3: The ecological impact of concrete components [7].*

For the sake of the simplicity, the three weighting coefficients $wc_\alpha = wc_\beta = wc_\gamma = 1$, and the impact of water is not considered (i.e., γ=1). Thus, Eq.(2) becomes:

$$EI = \alpha \cdot \beta \quad (3)$$

G. Habert, A. Schlueter (eds.): Expanding Boundaries © 2016 vdf Hochschulverlag AG an der ETH Zürich
DOI 10.3218/3774-6_67, ISBN 978-3-7281-3774-6, http://vdf.ch/expanding-boundaries.html

and the corresponding values of *EI*, referred to a cubic meter of the four series of concretes, are reported in Table 4.

| Series | EI<br>$kgCO_2$ MJ/m$^3$ |
|---|---|
| U_0 | 1.33E+07 |
| U_1 | 1.42E+07 |
| U_2 | 1.42E+07 |
| U_3 | 1.43E+07 |

*Table 4: The ecological index of the cement-based composites.*

### 2.2 Evaluation of MI

The mechanical performances of materials can be evaluated by considering the results of uniaxial tensile tests on dog bone samples (see Fig.2 [8]).

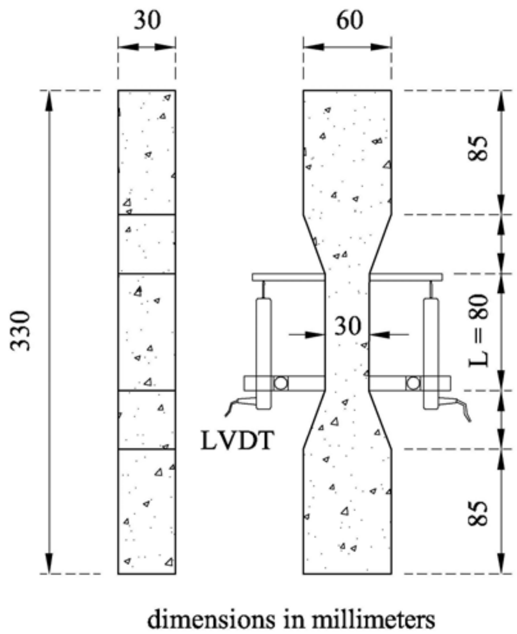


*Fig. 2: Geometrical properties of the "dumbbell type" specimens under uniaxial tension [8].*

The typical stress–strain relationship for UHP-FRCC under uniaxial tension is illustrated in Fig.3. In this figure, the symbol $\sigma_{fcs}$ represents the crack initiation stress, at which the first crack occurs, and $\sigma_{ts}$ represents the tensile strength. The average values of both the stresses, measured in the four series of concretes are reported in Table 5. In the same Table also the strain ($\varepsilon_{ts}$) at the tensile strength, generally considered as the strain capacity, is shown. In particular, it is the sum of the crack initiation strain ($\varepsilon_{fcs}$), and the inelastic strain up to the peak of stress. According to Naaman and Reinhardt [9], high-performance fiber-reinforced cement-based composites exhibit pseudo strain hardening with multiple cracks when $\sigma_{ts} \geq \sigma_{fcs}$ (see Fig.3).

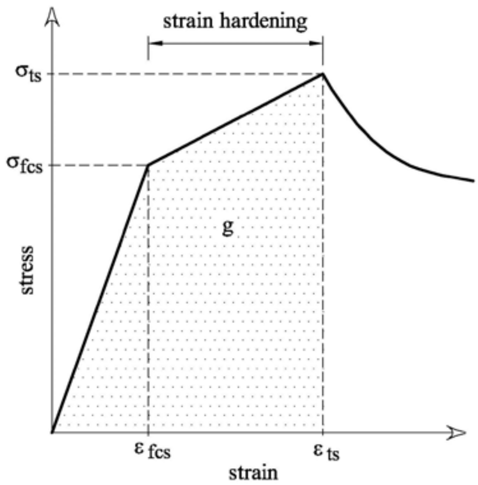


*Fig. 3: Strain hardening with multiple cracking in UHP-FRC.*

During the strain-hardening stage the energy absorption capacity (*g*) is defined as the area under the stress–strain curve from zero to $\varepsilon_{ts}$ (Fig.3). In UHP-FRCC the compressive strength is generally higher than 150 MPa and, in the pre-softening stage, the energy absorption capacity *g* is larger than 50 kJ/m$^3$ [3]. According to this definition, only U_0 cannot be considered as UHP-FRCC, as the absorption capacity is half of the lower bound value.

Depending on the application of the UHP-FRCC, one of the four parameters reported in Table 5 is assumed to be the mechanical index *MI*.

| Series | $\sigma_{fcs}$<br>MPa | $\sigma_{ts}$<br>MPa | $\varepsilon_{ts}$<br>% | *g*<br>kJ/m$^3$ |
|---|---|---|---|---|
| U_0 | 9.5 | 10.6 | 0.11 | 26 |
| U_1 | 12.5 | 14.6 | 0.74 | 112 |
| U_2 | 13.5 | 16.1 | 0.93 | 146 |
| U_3 | 13.8 | 16.2 | 1.16 | 156 |

*Table 5: Some of the mechanical parameters of the cement-based composites herein investigated.*

### 2.3 Eco-mechanical analyses

If $EI_{sup}$ and $MI_{inf1} = \sigma_{ts}$ are those of the control series U_0 (see Table 4 and Table 5), the non-dimensional diagram shown in Fig.4a is obtained.

G. Habert, A. Schlueter (eds.): Expanding Boundaries © 2016 vdf Hochschulverlag AG an der ETH Zürich
DOI 10.3218/3774-6_67, ISBN 978-3-7281-3774-6, http://vdf.ch/expanding-boundaries.html

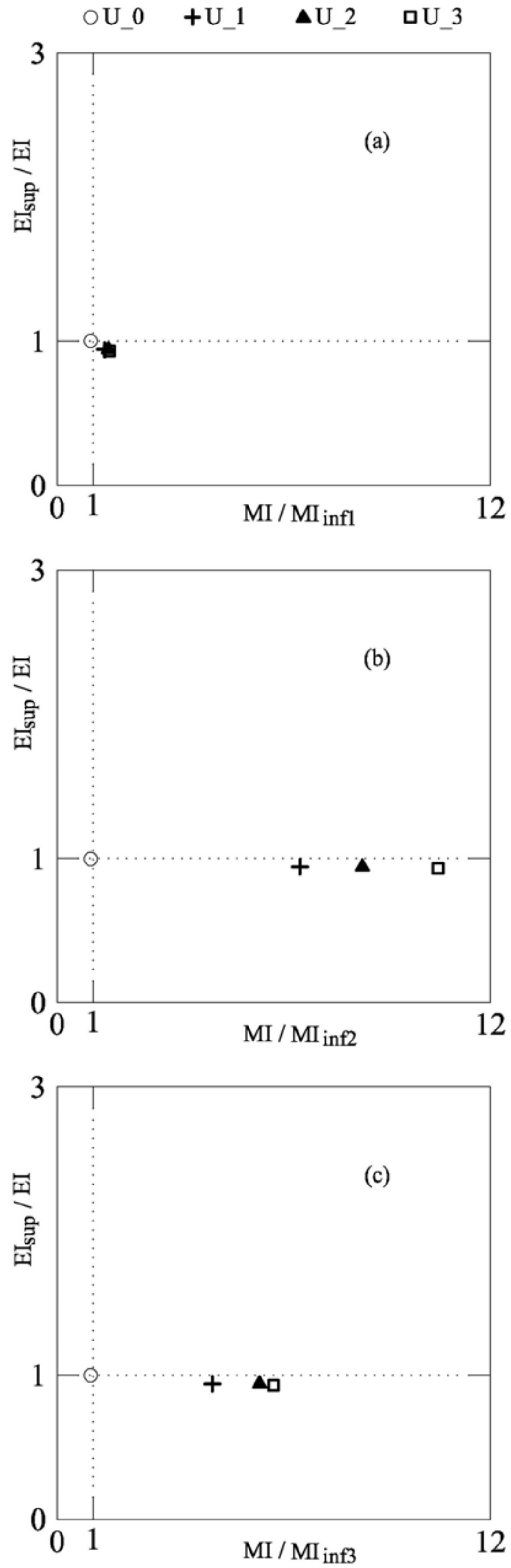


*Fig. 4: The non-dimensional diagrams referred to the mechanical properties of U_0: (a) $MI_{inf1} = \sigma_{ts}$ ; (b) $MI_{inf2} = \varepsilon_{ts}$ ; (c) $MI_{inf3} = g$.*

The analysis, performed at the material level (i.e., referred to a unit volume of U_0), does not reveal a great difference of *EI* and *MI* among the investigated composites (see Table 4 and the second column of Table 5). Whereas, a greater difference of the mechanical parameter can be observed when the other parameters reported in Table 5 are considered as *MI*. In fact, Fig.4b and Fig.4c show the comparisons in the case of $MI_{inf2} = \varepsilon_{ts}$ , and $MI_{inf3} = g$, respectively. Unfortunately, none of the UHP-FRCCs fall within zone 3 (Fig.1). Thus, a better comparison, especially in term of environmental impact, can be performed referring to a specific structure.

## 3 ANALYSIS AT STRUCTURAL SCALE

A simply supported concrete beam, having rectangular cross-section *b*×*h* , and subjected to a bending moment *M*, can be considered. The behaviour of the materials can be reproduced by the stress-strain constitutive relationship depicted in Fig.5. In addition to the bilinear response in tension (Fig.3), the linear response in compression is also assumed ($\sigma_{pc}$ = compressive strength, and $\varepsilon_{pc}$ = strain at $\sigma_{pc}$ ). To define this relationship in the four series, the data reported in Table 5 and Table 6 are both considered. With these properties, a cross-section of *b* =300 mm and *h* = 500 mm, and made with the control material U_0, can resist to a bending moment of *M* = 230 kN m.

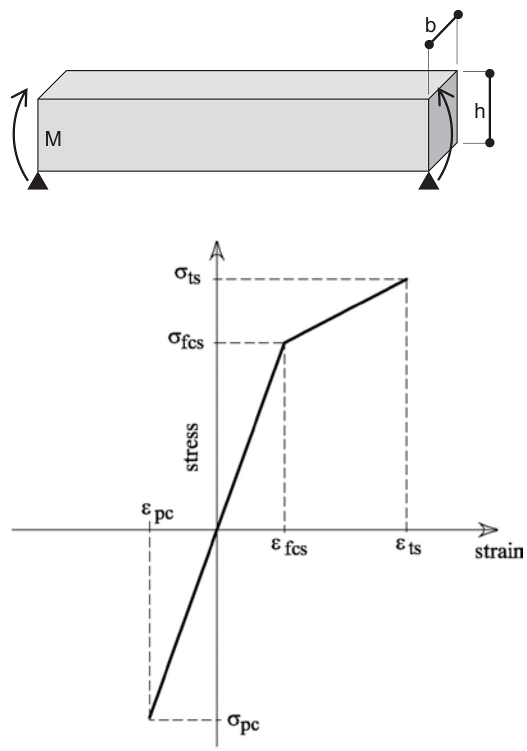


*Fig. 5: The complete stress-strain relationship of a beam made with UHP-FRCC.*

G. Habert, A. Schlueter (eds.): Expanding Boundaries © 2016 vdf Hochschulverlag AG an der ETH Zürich
DOI 10.3218/3774-6_67, ISBN 978-3-7281-3774-6, http://vdf.ch/expanding-boundaries.html

| Series | $\varepsilon_{fcs}$ % | $\sigma_{pc}$ MPa | $E_c$ GPa | $\varepsilon_{pc}$ % |
|---|---|---|---|---|
| U_0 | 0.059 | -211 | 510 | -0.41 |
| U_1 | 0.069 | -181 | 484 | -0.37 |
| U_2 | 0.065 | -187 | 490 | -0.38 |
| U_3 | 0.077 | -202 | 502 | -0.40 |

*Table 6: The main mechanical parameters of the cement-based composites herein investigated.*

If $h$ = 500 mm is constant, different values of $b$ can be obtained when the cross-sections have the same moment capacity (i.e., 230 kN) but are made with the concretes of the other series. Table 7 reports the values of $b$ and $h$ of all the cross-sections, whereas the corresponding moment-curvature relationships are illustrated in Fig.6.

| Series | b mm | h mm | EI $kgCO_2$ MJ/m |
|---|---|---|---|
| U_0 | 300 | 500 | 1.99 E+06 |
| U_1 | 161 | | 1.14 E+06 |
| U_2 | 144 | | 1.02 E+06 |
| U_3 | 140 | | 1.00 E+06 |

*Table 7: The geometrical dimensions of the cross-sections with a bending capacity of 230 kN m.*

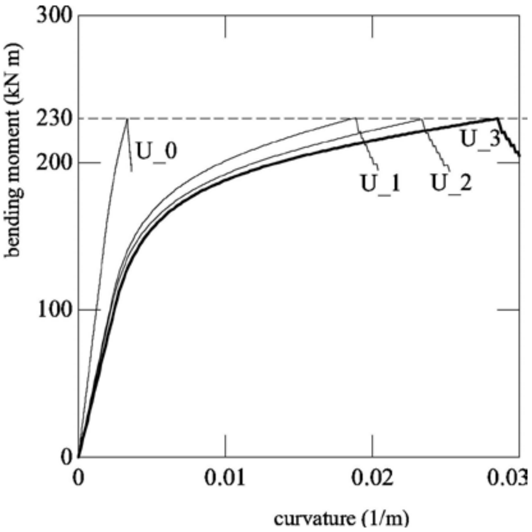


*Fig. 6: The moment-curvature relationship obtained in the four series of concrete analyzed herein.*

As shown in Fig.7a, all these diagrams can be approximated by a bi-linear relationship, in which the plastic part is limited by the maximum bending moment (i.e., $M$ = 230 kN m). Moreover, each bilinear diagram must define the same area with respect to the curvature axis. Accordingly, the first part of the bilinear moment-curvature can be calculated in order to have the area $A_1$ = $A_2$, as reported in Fig.7a. In the new bilinear diagrams, the larger the curvature in the plastic stage (i.e., $\Delta\mu$), the larger the ductility capacity of the cross-section.

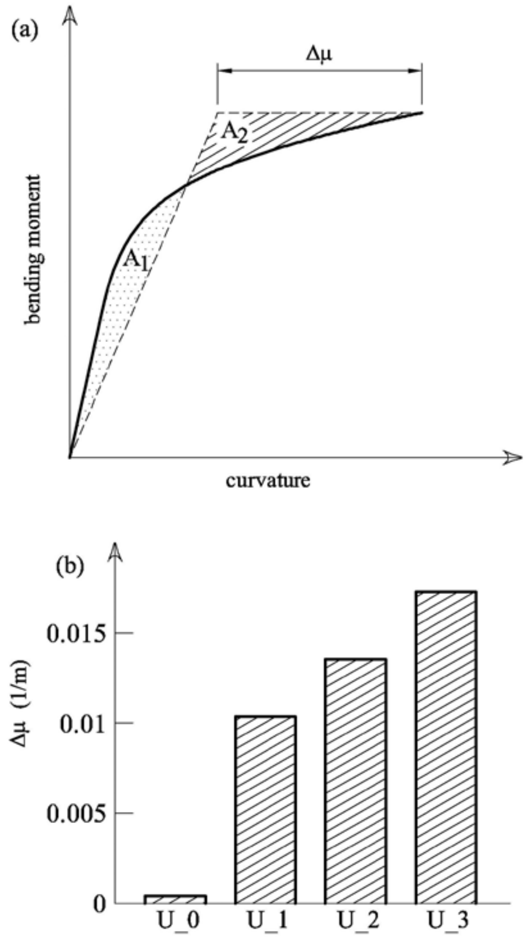


*Fig. 7: The ductility of the cross-sections: (a) bi-linearization of the moment-curvature relationship; (b) evaluation of ductility $\Delta\mu$.*

This is a fundamental mechanical property, especially for structures built in seismic areas. The values of $\Delta\mu$ reported in Fig.7b can be considered the mechanical index of each beam.

With respect to the control cross-section made with U_0, the use of wollastonite microfibers reduces the dimension and increases the ductility of the cross-section, without modifying the ultimate bending moment (see Table 7 and Fig.7b).

### 3.1 The eco-mechanical performances of beams

Thus, in concrete beams $MI = \Delta\mu$ can be considered. Whereas, the values of *EI* are those already evaluated in Table 4 multiplied by the area of each cross-section. In this way, *EI* is no longer related to the unit volume of the material, but to the unit length of the beam. Table 7 collects the new values of *EI.*

If $EI_{sup}$ and $MI_{inf4} = \Delta\mu$ are those of the control cross-section U_0, the new eco-mechanical

G. Habert, A. Schlueter (eds.): Expanding Boundaries © 2016 vdf Hochschulverlag AG an der ETH Zürich
DOI 10.3218/3774-6_67, ISBN 978-3-7281-3774-6, http://vdf.ch/expanding-boundaries.html

analysis can be performed, as reported in the non-dimensional diagram of Fig.8.

Although all the UHP-FRCCs fall within zone 3, the best performances are those of the series U_3, because such concrete shows the best ecological (i.e., the lowest *EI* in Table 7) and mechanical (i.e., the highest *MI* in Fig.7b) performances when it is used in beams subjected to bending moment. Conversely, at the material level (see Table 4), U_3 has the highest *EI*, or the highest environmental impact.

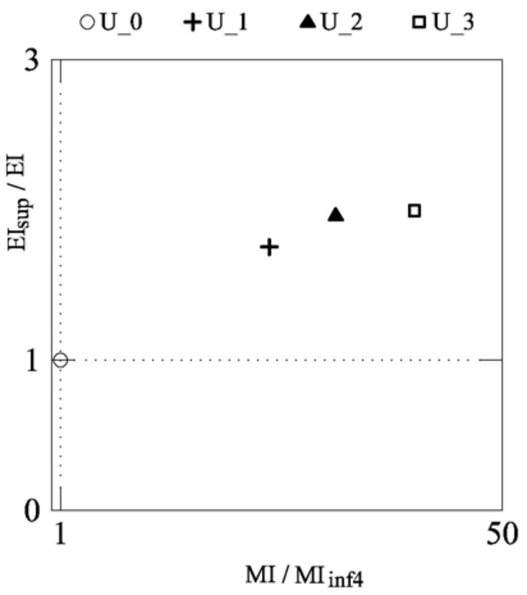


*Fig. 8: The non-dimensional diagram referred to the mechanical properties of the beam U_0 and to $MI_{inf4} = \Delta\mu$.*

## 4 SUMMARY

According to the results of both the theoretical and experimental analyses previously described, the following conclusions can be drawn:

- Both the ecological and mechanical performances have been measured conjunctly at material and structural scales.
- If only the mechanical properties of materials are taken into account, UHP-FRCCs made with wollastonite microfibers behave better than FRCC only in terms of mechanical performances.
- If the structural behaviour (i.e., strength and ductility) of a beam in bending are taken into account, UHP-FRCCs containing wollastonite microfibers behave better than FRCC.

As a general conclusion, the presence of wollastonite makes the UHP-FRCC more ductile and sustainable, thus a large use of this material in the concrete structures is desirable.

## 5 REFERENCES

1. Fantilli, A.P. and Chiaia B. Eco-mechanical performances of cement-based materials: an application to self-consolidating concrete. Construction & Building Materials, 2013. 40: pp. 189–196.

2. Fantilli, A.P. and Chiaia, B. The work of fracture in the eco-mechanical performances of structural concrete. Journal of Advanced Concrete Technology, 2013. 11: pp. 282-290.

3. Wille, K., El-Tawil, S. and Naaman, A.E. Properties of strain hardening ultra high performance fiber reinforced concrete (UHP-FRC) under direct tensile loading. Cement & Concrete Composites, 2014. 48: pp. 53–66.

4. Kwon, S., Nishiwaki, T., Choi, H. and Mihashi, H. Effect of Wollastonite Microfiber on Ultra-High-Performance Fiber-Reinforced Cement-Based Composites Based on Application of Multi-Scale Fiber-Reinforcement System. Journal of Advanced Concrete Technology, 2015. 13 (7): pp. 332-344.

5. Habert, G. and Roussel, N. Study of two concrete mix-design strategies to reach carbon mitigation objectives. Cement and Concrete Composites, 2009. 31: pp. 397–402.

6. *fib*. Guidelines for Green Concrete Structures, in *fib* bulletin N. 67, 2012. International Federation for Structural Concrete: Lausanne.

7. Chiaia, B., Fantilli, A.P., Guerini, A., Volpatti, G. and Zampini D. Eco-mechanical index for structural concrete. Construction and Building Materials, 2014. 67 (Part C, 30): pp. 386-392.

8. Japan Society of Civil Engineers. Recommendations for Design and Construction of HPFRCC with Multiple Fine Cracks, 2008. (http://www.jsce.or.jp/committee/concrete/e/hpfrcc_JSCE.pdf ).

9. Naaman, A. E. and Reinhardt, H. W. Characterization of high performance fiber reinforced cement composites-HPFRCC, in 'High Performance Fiber Reinforced Cement Composites 2.1995: Ann Arbor, pp. 1-24

G. Habert, A. Schlueter (eds.): Expanding Boundaries © 2016 vdf Hochschulverlag AG an der ETH Zürich
DOI 10.3218/3774-6_67, ISBN 978-3-7281-3774-6, http://vdf.ch/expanding-boundaries.html